International Journal of Pharmaceutics 401 (2010) 72–78

Contents lists available at ScienceDirect

International Journal of Pharmaceutics

journal homepage: www.elsevier.com/locate/ijpharm

Pharmaceutical Nanotechnology

Nanogel particulates located within diffusion cell receptor phases following topical application demonstrates uptake into and migration across skin

Nor Abu Samah, Nicholas Williams, Charles M. Heard *

Welsh School of Pharmacy, Cardiff University, Cardiff CF10 3NB, UK

ARTICLE INFO

Article history:
Received 14 May 2010
Received in revised form 2 August 2010
Accepted 5 August 2010
Available online 15 September 2010

Keywords:
Nanogel
PolyNIPAM
Topical drug delivery
Skin
Transmission electron microscopy
Methotrexate

ABSTRACT

Despite growing evidence in support of nanogels as carriers in topical drug delivery, no empirical evidence has been forthcoming regarding a mechanism. Poly(*N*-isopropylacrylamide-copolymerized-acrylic acid) referred to as poly(NIPAM-*co*-AAc) and poly(*N*-isopropylacrylamide) known as (polyNIPAM) nanogels were synthesized by a surfactant-free emulsion polymerisation method and applied to porcine ear skin mounted in Franz diffusion cells. After 24 h the receptor phases were retrieved and scrutinized by transmission electron microscopy (TEM). The skin membranes were also recovered and re-used to determine the permeation of a model permeant, methotrexate (MTX). TEM images confirmed the presence of nanoparticulates in the receptor phases, and the relative quantities varied on the nature of the nanogel. Comparative MTX skin permeation data demonstrated the integrity of the membranes, and that delivery of nanogel or MTX was not due to defects in the membranes. In summary, the first direct evidence is presented demonstrating that nanogels are taken up by and migrate across the skin.

1. Introduction

Nanogels are nano-sized networks of chemically or physically crosslinked polymer particles. Depending on the chemical nature of the monomers used, the polymer swells in a particular solvent under specific environmental stimuli such as temperature, pH, ionic strength and quality of solvent, then undergoing rapid conformational changes and releasing the solvent again following changes in environmental stimuli (Das et al., 2006; Don et al., 2008; Galaev and Mattiasson, 2007). The swollen nanogel particles contain considerable amount of aqueous solvent and are typically ranging in diameter from 100 to 1000 nm at ~25 °C (Das et al., 2006).

In this work, attention was focused on poly(*N*-isopropylacrylamide) (herein referred to as polyNIPAM), the most well-established smart polymer (Galaev and Mattiasson, 2007). *N*-isopropylacrylamide (NIPAM), the major building block of this polymer, exhibits temperature-dependant particle size and has a high monodispersity of particle size distribution (Saunders, 2004). The crosslinked polyNIPAM nanogel usually undergoes volume collapse due to expulsion of its content at a certain temperature known as volume phase transition temperature (VPTT) (Saunders, 2004). Generally, the VPTT value is close to the lower critical solution temperature (LCST) of the corresponding solution of a non-crosslinked polymer (Schmidt et al., 2005). The experimental LCST value of a linear form polyNIPAM polymer in aqueous solvent is ~32 °C and when the NIPAM is crosslinked into a polyNIPAM gel by a crosslinker agent, its VPTT is between 32 and 35 °C (Hoare and Pelton, 2004). PolyNIPAM nanogels can be customized to possess certain desired properties by varying the monomers used during synthesis. The combination of monomers, which respond to different stimuli or have ranging hydrophobicity properties, creates nanogels that exhibit physico-chemical properties which are composite of those of the co-monomers employed in their preparation (Galaev and Mattiasson, 2007; Oh et al., 2008). These unique features are found to be diversely beneficial in pharmaceutical, biotechnology and biomedical applications (Galaev and Mattiasson, 2007).

The use of nanoparticles is currently of great interest as 'smart' carriers in a range of drug delivery areas, including topical delivery (de Jalón et al., 2001; Lademann et al., 2008; Leslie Singka et al., in press). Despite a growing body of evidence demonstrating the efficacy of nanoparticles in topical drug delivery, a mechanism remains to be established, as does any definitive evidence that such particles either penetrate or permeate the skin. Investigations carried out so far centre on the use of biophysical techniques to image nanoparticles loaded with fluorescent probe within the skin, e.g. confocal microscopy, and these have so far been of limited success (Toll et al., 2003; Alvarez-Román et al., 2004; Wu et al., 2009). In the current work, we took the view that if nanogels indeed penetrate into the stratum corneum or appendages then ultimately, they could be expected to migrate all the way across the skin. In

* Corresponding author. Tel.: +44 029 20875819; fax: +44 029 20874149.
E-mail address: heard@cf.ac.uk (C.M. Heard).

0378-5173/$ – see front matter © 2010 Elsevier B.V. All rights reserved.
doi:10.1016/j.ijpharm.2010.08.011

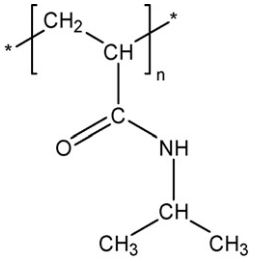

Fig. 1. Chemical structure of polyNIPAM.

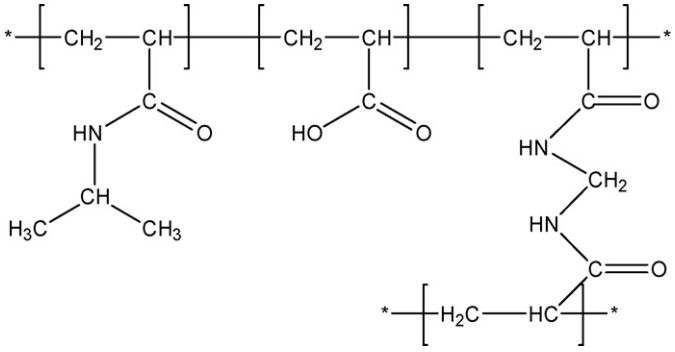

Fig. 2. Chemical structure of poly(NIPAM-*co*-AAc).

an *in vitro* setting, it should therefore be possible to locate them within the receptor phases of diffusion cells.

Two types of nanogel were synthesized for this investigation: (1) temperature-sensitive polyNIPAM (Fig. 1) treated as a control and (2) temperature-sensitive polyNIPAM modified using acrylic acid (AAc, ionic co-monomer) to yield particles with pH-responsive swelling properties, poly(NIPAM-*co*-AAc) (Fig. 2). The first phase involved the application of swollen nanogel particles onto porcine heat separated epidermal membranes installed in glass Franz diffusion cells. After 24 h, the receptor phases were retrieved and analyzed by transmission electron microscopy (TEM) imaging. The second part of the investigation was carried out with the aim of validating the integrity of the epidermal membranes post-treatment with the nanogels. To this end, the membranes were re-used and the permeation of a model drug, methotrexate (MTX) determined under several conditions.

2. Materials and methods

2.1. Materials

NIPAM (99%), and potassium persulfate ($K_2S_2O_8$, 99.9%), glass wool and high performance liquid chromatography (HPLC)-grade solvents were purchased from Fisher Scientific (Loughborough, UK). AAc (99%), citric acid anhydrous (CA, 99.5%), Hanks' balanced salts solution (HBSS), *N*,*N*′-methylenebis-acrylamide (MBA), phosphate buffered saline solution (PBS, pH 7.4), potassium phosphate monobasic and Whatman™ qualitative filter paper Grade 4 were all purchased from Sigma–Aldrich Company Ltd. (Poole, UK). MTX was obtained from Heumann PCS GmBH (Feucht, Germany). Freshly excised porcine ears were obtained from a local abattoir prior to steam cleaning and immersed in iced HBSS upon excision.

2.2. Nanogel synthesis

Poly(NIPAM-*co*-AAc) and polyNIPAM nanogels were synthesized by a single-step surfactant-free emulsion polymerisation (SFEP) reaction according to the recipes given in Table 1. NIPAM, MBA and de-ionised water were added together in a beaker and stirred for ~15 min on a magnetic stirrer plate. The mixture was continuously stirred in a 250-mL three-neck round-bottom flask equipped with a magnetic stirrer bar and immersed in a water bath heated to the polymerisation temperature of ~70 °C. The flask was continuously purged with nitrogen gas to maintain anoxic conditions. For the poly(NIPAM-*co*-AAc) nanogel synthesis, AAc was added at a concentration of 5% w/v to the base monomer mixture ~15 min prior to the addition of a hot pre-dissolved persulfate initiator (made-up before hand in 100-mL of de-ionised water). The colour of the solution turned sky blue from transparent until it reached an ivory white indicating successful polymerisation (Pelton and Chibante, 1986; Lin et al., 2006). The polymerisation proceeded for 6 h under continuous 300 rpm mixing, and the mixture was cooled overnight under constant stirring, before being filtered by a combination of glass wool and a filter paper to remove any large clumps. Residual monomers and other impurities were removed by centrifugation, involving five cycles of centrifugation (Beckman Coulter Avanti-J25, 50,000 × *g* for 1 h at 20 °C a cycle), decantation and re-dispersion in de-ionised water. For ease of storage and handling purposes, the concentrated nanogels were subjected to freeze drying for ~48 h. The freeze-dried samples were stored in a refrigerator (~4 °C) until use.

2.3. Nanogel characterisations

2.3.1. Temperature and pH-responsive effects

The purified nanogel particles were characterized at ambient temperature using a laser diffraction system Malvern *Mastersizer 2000*™ (Malvern Instruments Ltd., Malvern, UK). Nanogels possess the ability to swell in specific solutions and therefore each preparation was prepared in the polymerisation solvent system (de-ionised water). Nanogel dispersions of 0.1% w/v were prepared by a dilution of the stock dispersions in clean-capped vials. The samples were stored at different temperatures: 4 °C (refrigerator – storage condition for the nanogels), 25 °C (room temperature – temperature during nanogels handling and analysis), 32 °C (average skin surface temperature), 37 °C (physiological temperature), 50 and 60 °C, allowing at least 1 h for temperature equilibrium. For the Mastersizer analysis, de-ionised water was used as the dispersant medium and treated the same as each test sample. Each sample was analyzed in triplicate ($n = 3$).

The response of nanogels to pH was also investigated. Solutions of variable pH values (~pH 2, 4, 5.8, 6, 8, and 10) were prepared through drop-wise addition of either HCl (0.1 M) or NaOH (0.1 M), monitored using a digital pH meter (PH209 Bench pH Meter, Hanna Instruments Ltd., UK). Nanogel dispersions of 0.1% w/v were prepared by mixing the freeze-dried nanogels in the solutions of variable pH using a laboratory flask shaker (Stuart™ Flask Shaker – SF1 *Bibby Scientific Ltd.*, Staffordshire, UK) for 30 min. pH of the resulting dispersions was not adjusted any further. The dis-

Table 1
Preparation of polyNIPAM and poly(NIPAM-*co*-AAc) nanogels for 250 mL preparations.

Nanogel	NIPAM (g)	AAc (mL)	MBA (g)	$K_2S_2O_8$ (g)	Stirring rate (rpm)
Poly(NIPAM-*co*-AAc)	2.5	0.12	0.0625	0.0475	300
PolyNIPAM (control)	2.5	–	0.0625	0.0475	300

persions were left to equilibrate at room temperature for another 30 min prior to analysis using the Malvern Mastersizer 2000™. Measurements were performed in triplicate at room temperature ($n = 3$).

The fundamental size distribution derived by this technique was volume based and expressed in terms of the volume of equivalent spheres ($D_{N\%}$) and weighted mean of the volume distribution (mass mean diameter). As the laser diffraction system was used for the analysis, two values that would give a rough equivalent on particle polydispersity are uniformity (how symmetrical the distribution is around the median point) and span (the width of the distribution). The span value, defined as below:

$$\text{Span} = \frac{D_{90\%} - D_{10\%}}{D_{50\%}} \quad (1)$$

where $D_{N\%}$ ($N = 10, 50, 90$) means that the volume percentage of particles with diameters up to $D_{N\%}$ equals to $N\%$. The smaller the span value the narrower the particle size distribution.

2.3.2. Phase transition determination: differential scanning calorimetry (DSC)

DSC analysis was done using a Perkin-Elmer DSC 7 differential scanning calorimeter/TAC-7 thermal analysis controller with an IntraCooler-2 cooling system (Perkin-Elmer Instruments, USA). Thermal Data Analysis Pyris software package (version 9.0.1.0174) for Windows supplied by the instrument manufacturer was used for data acquisition and analysis. Samples were prepared by immersing ~10 mg of dried polymer in 500 μL of de-ionised water. All samples were equilibrated at ~4 °C for 24 h and concentrated by centrifugation (Beckman Coulter Avanti-J25, 50,000 × *g* for 1 h at 20 °C) prior to measurements. Approximately 10 μl of each swollen sample transferred by pipette into an aluminium pan and then sealed by an aluminium lid. Polymer-free solutions of the same solvent composition were placed in the reference pan. The thermal analyses were performed on the swollen polymers from 5 to 70 °C at a scanning rate of 5 °C min^{-1}, using nitrogen as blanket gas. The calorimeter asymmetry between the empty reference and sample calorimeters was eliminated with an empty-pan run used as a baseline for the heat-flow rate of the sample and calibration runs. The LCST value (average of two measurements) was arbitrarily taken as the abscissa of the maximum of the endothermic transition peak.

2.4. In vitro migration of nanogel particles across epidermal membranes

Nanogels samples were prepared as aqueous dispersions (10% w/v), which were left to equilibrate for 24 h (to attain maximize swelling) and concentrated by a centrifugation method (Beckman Coulter Avanti-J25, 50,000 × *g* for 1 h at 20 °C). The resulting gels were kept refrigerated at ~4 °C prior to use.

The porcine ears were cleaned under running water and full thickness skin excised from the dorsal side by blunt dissection using a scalpel. Any hairs were trimmed using electric clippers, prior to being cut into sections of approximately 3 × 3 cm then immersed in water heated to ~60 °C for approximately 1 min. Epidermis was then carefully liberated with the aid of forceps and examined by magnifying glass to check for any physical damage prior to use. The epidermal membrane sections were mounted onto pre-greased receptor compartments of scrupulously clean glass Franz-type diffusion cells with the stratum corneum side facing upwards. Pinch clamps were affixed and the receptor compartments filled with temperature-equilibrated de-ionised water (receptor phase) using a syringe. Micro-magnetic stirrer bars were added and the complete assemblies placed on a submersible magnetic stirring plate (Variomag, Daytona Beach, USA) set up in a water bath maintained at ~37 °C, providing a skin surface temperature of ~32 °C. After 15 min, nanogels were applied to the surface of the skin using a pipette and then a blunt glass rod was used to gently (20 circular motions) massage the sample onto the membranes. Both the sampling arm and donor compartments were occluded. Three replicates were prepared for each nanogel samples ($n = 3$). Five dosing procedures were used:

1. 500 μL polyNIPAM nanogel (10% w/v) alone.
2. 500 μL poly(NIPAM-*co*-AAc) nanogel (10% w/v) alone.
3. 500 μL poly(NIPAM-*co*-AAc) nanogel followed by 200 μL CA solution (50 mg mL^{-1}, ~pH 1.9).
4. 200 μL CA solution (50 mg mL^{-1}) alone.
5. 500 μL de-ionised water alone.

Membranes dosed with the polyNIPAM nanogel acted as a control for the copolymerized poly(NIPAM-*co*-AAc) nanogel. In addition, CA solution was added together with the poly(NIPAM-*co*-AAc) nanogel as a pH modulator for the nanogel particles. Furthermore, some membranes were dosed with the CA solution alone in order to determine whether the pH modulator could cause any damage to the skin barrier. Membranes treated with de-ionised water were used as an overall control. After 24 h the cells were dismantled and the receptor phases retrieved by individual Pasteur pipettes and immediately analyzed by TEM. The membranes were also retained for validation of membrane integrity.

2.5. TEM analysis

Receptor phases were scrutinized for the presence of nanogel particles using a Phillips EM 208 instrument operated at 80 kilovolts (kV). Approximately 10 μL of the samples was transferred using a pipette onto 200- mesh size Pioloform™ -coated copper grids. A negative stained technique with uranyl acetate (UA, 2% w/v) was used in order to enhance particles visualization by increasing image contrast. In order to minimize any loss of particles on the grids, the samples were not washed with distilled water. At least five micrographs were taken for each sample ($n = 5$). Quantitative measurements of TEM micrographs were laboriously performed using a digital image processing program known as ImageJ (Image processing and analysis in JAVA, version 1.43f, National Institute of Health, USA).

2.6. Membrane integrity validation: in vitro permeation of MTX

A saturated solution of MTX was prepared by adding excess into 15 mL of de-ionised water in an amber glass bottle until no further dissolution was observed visually. The mixture was loaded on a rotary blood cell mixer and left to equilibrate for 24 h at room temperature. Afterwards, it was subjected to centrifugation (Beckman Coulter Avanti-J25, 5 000 × *g* for 1 h) and the supernatant was sampled and used immediately. *In vitro* skin permeation was generally carried out according to the method outlined earlier. The membranes were carefully recovered from the previous permeation test and gently cleaned with soft tissues before being re-mounted in the glass Franz diffusion cells. A receptor phase of PBS was used to provide sink conditions for MTX. Each membrane was dosed with 500 μL of the saturated solution of MTX (0.17 ± 0.001 mg mL^{-1}, ~pH 7.3) using a pipette and rubbed gently using a glass rod (~20 circular motions). After 24 h, the receptor phases were collected and immediately assayed for MTX.

2.7. Quantitative analysis of MTX

Samples were analyzed by reverse-phase liquid chromatography using an Agilent 1100 series automated system with Chemstation™ software. The HPLC method was developed in-

house: Reverse phase HPLC column Gemini^{TM}-NX C18 ODS (250 mm × 4.6 mm, 5 μm) with a SecurityGuard^{TM} guard cartridge (Phenomenex, UK), mobile phase of 3:1 potassium phosphate buffer (0.1 M, pH 6.5)/methanol over 15 min with flow rate set at 1 mL min^{-1}. Sample injection volume was 20 μL and detection was by UV at λ = 305 nm, with a resultant MTX retention time of 9 min. As the saturated solution of MTX was prepared in de-ionised water and PBS was used as the receptor phase of the permeation test, two calibration curves were developed. Standard calibration curves obtained over the range of 0.8–200 μg mL^{-1} and linearity were good as evidenced by R^2 of 0.99 with a limit of detection of 0.2 μg mL-1 (PBS) and 8.3 μg mL^{-1} (de-ionised water).

2.8. Data analysis

The data obtained were collected and analyzed using Excel 2007 (Microsoft Office, Microsoft Inc., US) and expressed as a mean ± standard deviation (S.D.). Statistical tests were performed with InStat3 for Mac (GraphPad Software Inc., Elysian, US). Significant differences and comparisons were made using one-way analysis of variance (ANOVA). Confidence interval was 95% with $p < 0.05$ considered as significant.

3. Results and discussion

3.1. Characterisation of nanogels particles

Since the poly(NIPAM-*co*-AAc) and polyNIPAM contained NIPAM component, it was anticipated that the nanogels would respond towards temperature stimulus. Each nanogel underwent thermally induced de-swelling event when the solution temperature was increased gradually from 4 to 60 °C (Fig. 3). The poly(NIPAM-*co*-AAc) particles were found to be significantly larger

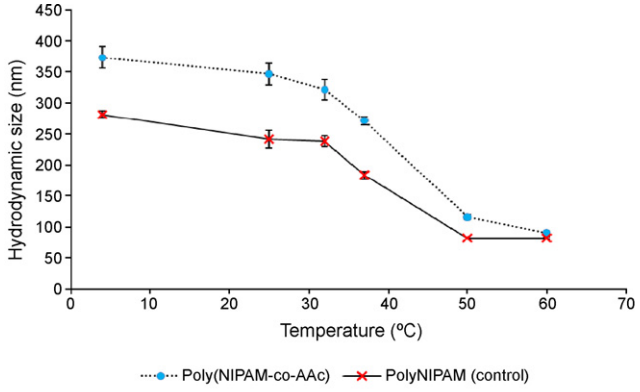

Temperature (°C)	Poly(NIPAM-*co*-AAc)		PolyNIPAM	
	Span	Uniformity	Span	Uniformity
4	0.610 ± 0.005	0.194 ± 0.004	0.796 ± 0.042	0.253 ± 0.011
RT (~25)	0.635 ± 0.033	0.200 ± 0.012	0.837 ± 0.055	0.266 ± 0.017
32	0.612 ± 0.002	0.195 ± 0.001	0.789 ± 0.003	0.245 ± 0.003
37	0.616 ± 0.018	0.274 ± 0.018	0.833 ± 0.039	0.261 ± 0.012
50	0.726 ± 0.042	0.229 ± 0.015	0.568 ± 0.002	0.180 ± 0.001
60	0.589 ± 0.001	0.176 ± 0.001	0.574 ± 0.004	0.181 ± 0.002

Fig. 3. Temperature dependence of poly(NIPAM-*co*-AAc) and polyNIPAM (control) nanogels particles presented as an average hydrodynamic size measured by laser light diffraction method ($n = 3$). Error bars represent standard deviation (S.D.). Span and uniformity values represent polydispersity of the particles.

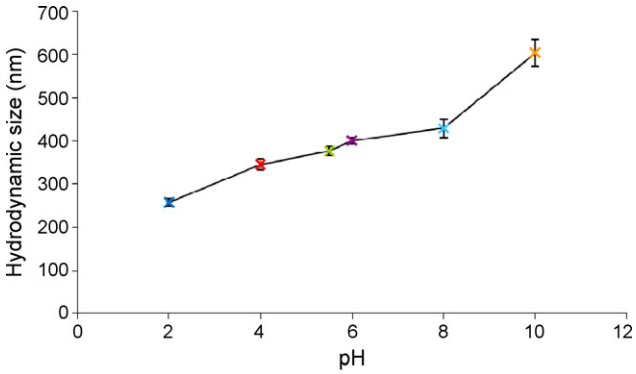

pH	Span	Uniformity
2	1.072 ± 0.174	1.007 ± 1.009
4	0.790 ± 0.059	0.251 ± 0.028
5.5	0.638 ± 0.003	0.203 ± 0.001
6	0.699 ± 0.001	0.217 ± 0.001
8	0.784 ± 0.015	0.263 ± 0.037
10	0.563 ± 0.018	0.178 ± 0.001

Fig. 4. pH dependence of the hydrodynamic sizes of poly(NIPAM-*co*-AAc) nanogel particles measured at ambient temperature. Data presented as an average hydrodynamic size ($n = 3$) and error bars represent standard deviation (S.D.). Span and uniformity values represent polydispersity property of the particles.

than the polyNIPAM particles ($p = 0.0013$) at room temperature. The average hydrodynamic sizes for poly(NIPAM-*co*-AAc) and polyNIPAM nanogel particles were found to be, 346 ± 17 and 242 ± 14 nm, respectively. The further expansion of the poly(NIPAM-*co*-AAc) nanogel matrix in comparison to the control can be explained by increased uptake of water as a result of the incorporation of a hydrophilic AAc co-monomer (Lee et al., 2008).

Incorporation of a co-monomer containing acidic functionality (AAc) into polyNIPAM nanogel yields poly(NIPAM-*co*-AAc) particles with pH-driven swelling property. It was found that the hydrodynamic size of poly(NIPAM-*co*-AAc) nanogel particles increased with a corresponding rise in pH as shown in Fig. 4. Variations in solution pH generate a change in the polymer network ionisation which further induced a change in its swelling capacity. The polymeric networks of poly(NIPAM-*co*-AAc) contain carboxylic acid groups which may ionize when the pH of the external environment rises above the pK_a of the AAc moieties (pK_a at 25 °C = 4.25). The polymer has a compact conformation below its pKa and a more extended conformation above, because of intramolecular charge repulsion effects between the ionized AAc residues within the polymer networks. On the other hand, no pH effect was observed for the polyNIPAM nanogel because it contains a very low density of ionisable groups originating from the persulfate initiator (data not shown).

For the hydrodynamic size study, the polydispersity of each sample was evaluated based on span and uniformity values which overall are considered to be in a narrow range (Figs. 3 and 4). The size and shape uniformity of nanogels particles can also be confirmed visually based on the TEM images. Fig. 5 shows the poly(NIPAM-*co*-AAc) and polyNIPAM particles to be monodisperse spheres having a regular size and shape with narrow size distributions.

Fig. 6 shows that the LCST for poly(NIPAM-*co*-AAc) in-deionised water was 31.1 °C with a wide transition temperature range, whereas the LCST for the polyNIPAM (control) was 31.8 °C with

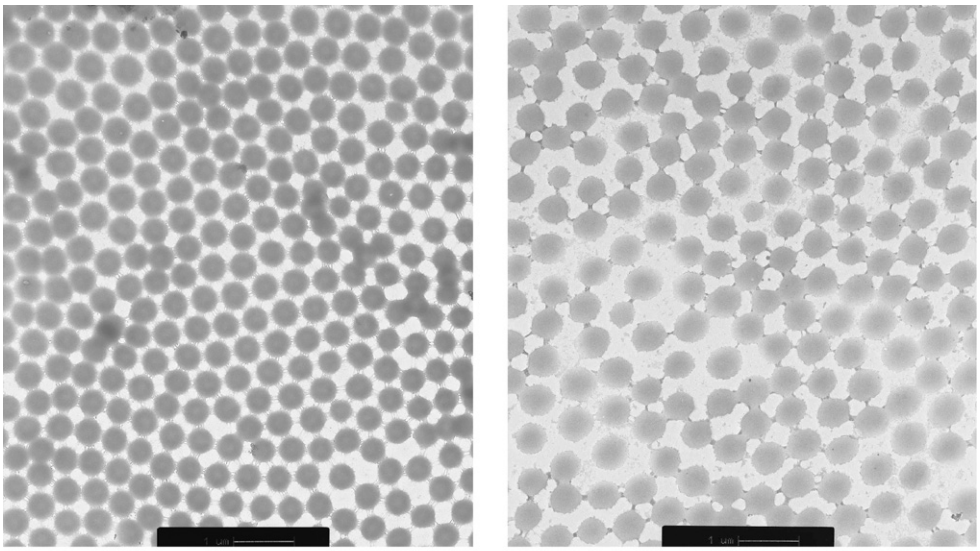

Fig. 5. TEM images of purified polyNIPAM and poly(NIPAM-*co*-AAc) nanogels particles. Samples were prepared in de-ionised water (0.1% w/v) and stained with UA (2% w/v) prior to the imaging. Scale bar: 1 μm.

a narrow transition range. Even though it may be expected that the incorporation of a hydrophilic monomer (AAc) would increase the temperature range over which the de-swelling event takes place, the presence of the carboxylic acid group did not significantly affect the de-swelling transition of the resulting polymer, as previously reported (Dowding et al., 2000).

3.2. Evidence of nanogels particles in receptor phase

For the TEM analysis, the content of each receptor phase was considered to be uniformly distributed across the TEM grid during the sample preparation. The grid was assumed to have an equal size of squares (200 squares per grid), thus no specific unit was assigned for each square. Nanoparticles of polyNIPAM and poly(NIPAM-*co*-AAc) were observed in the samples indicating delivery of nanogels beyond the epidermis layer, as shown in Fig. 7. A trend can be seen in which fewer polyNIPAM nanogel particles migrated across the epidermal membrane in comparison to the poly(NIPAM-*co*-AAc). Although the rules for permeation of small molecules clearly do not apply to nanoparticulates, it can be assumed that the greater the hydrodynamic diameter the more arduous the migration process. Fig. 8 shows the relative quantities of nanogel particles detected in the receptor phases, after 24 h. There was a significant difference in particle migration between the polyNIPAM and poly(NIPAM-*co*-AAc) ($p = 0.0434$). The trend may be explained as the polyNIPAM particles are only responsive towards a thermal stimulus (32 °C, average skin surface temperature) whereas the poly(NIPAM-*co*-AAc) particles are responsive towards thermal and pH stimuli (skin surface temperature and pH) as previously discussed in the characterization (Section 3.1). In this work, poly(NIPAM-*co*-AAc) nanogel was designed to be a carrier for topically applied drugs. In principle, the nanogel particles should experience volume collapse by expulsion of their contents at a temperature close to the average surface skin temperature (32 °C) in comparison to the typical storage condition (25 °C). Over the temperature range, the poly(NIPAM-*co*-AAc) particles experienced de-swelling by only 7.2% which was considered not significant ($p = 0.1448$). Even though the thermal responsive behaviour of the nanogel particles was not significant, it still offered a minor contribution to the overall size reduction of the particles. Thus, the enhanced migration effect might be largely accounted for by its pH-responsive property. Variable skin pH values have been reported, all in the acidic broad range from pH 4.0 to 7.0 (Lambers et al., 2006). In response towards the acidic environment of the skin, the poly(NIPAM-*co*-AAc) nanogel particles might

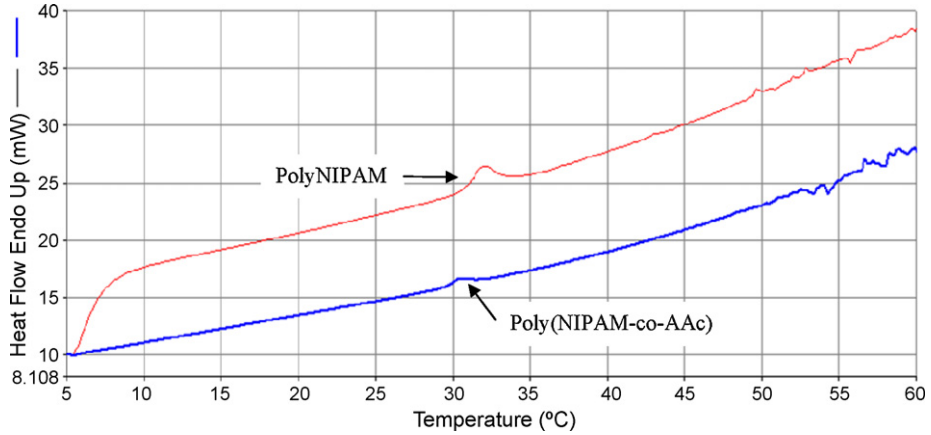

Fig. 6. DSC traces of swollen poly(NIPAM-*co*-AAc) and polyNIPAM nanogels for determining their LCST. The onset point of the endothermal peak, determined by the intersecting point of two tangent lines from the baseline and slope of the endothermic peak, was used to determine the LCST.

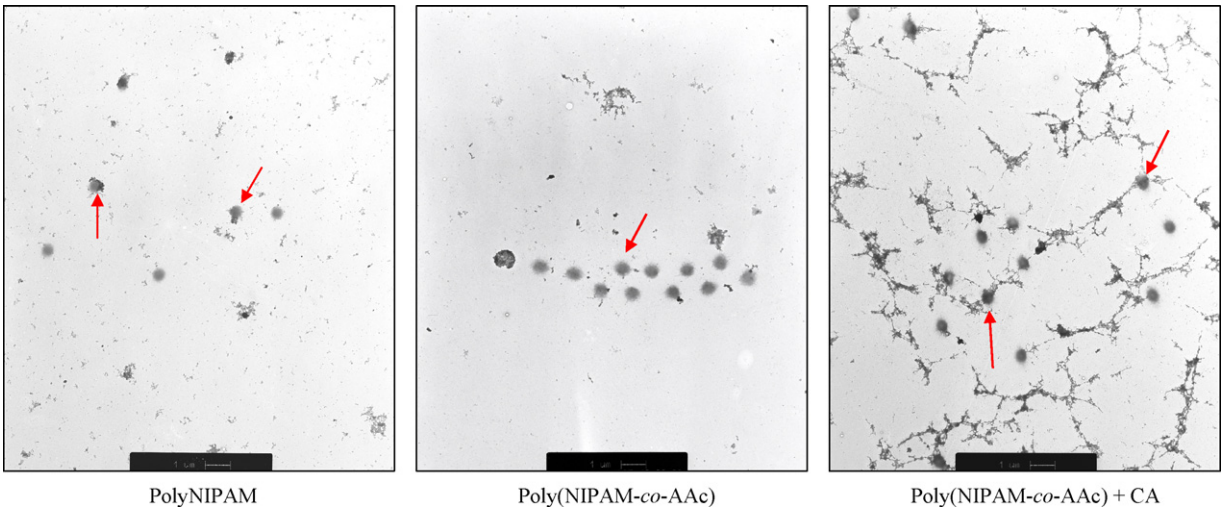

Fig. 7. TEM images of nanogels particles observed in the receptor phases collected after 24 h. Scale bar: 1 μm.

have experienced further shrinkage (smaller size) due to the expulsion of their content.

Effect of an external pH modulator on permeation of the blank poly(NIPAM-*co*-AAc) particles was also investigated. According to the characterization study of the nanogel, an acidic pH modulator may trigger further de-swelling of the particles. We chose CA as the acidic modulator for the corresponding nanogel as this compound is widely used in consumers' cosmetic products. Since the pH modulator used in this study had a pH value roughly around 1.9, and the nanogel was prepared in de-ionised water of pH 5.8, the particles were expected to experience a very significant size reduction of 32% over this range ($p = 0.0002$) as shown in Fig. 4. However, based on the results obtained in Fig. 8, its application onto the poly(NIPAM-*co*-AAc) nanogel contributes only a minor effect on the permeation of the ionic nanogel particles as there was no significance difference reported with or without the addition of the CA solution ($p = 0.3659$).

3.3. Validation of skin membrane integrity post-application of nanogels

As nanogels have such a low hydrodynamic size, any breeches or defects in the membrane would be liable to yield false positives in terms of nanoparticles appearing in the receptor phase, not having migrated through the intact barrier function of the skin. The purpose of this experiment was therefore to validate the integrity

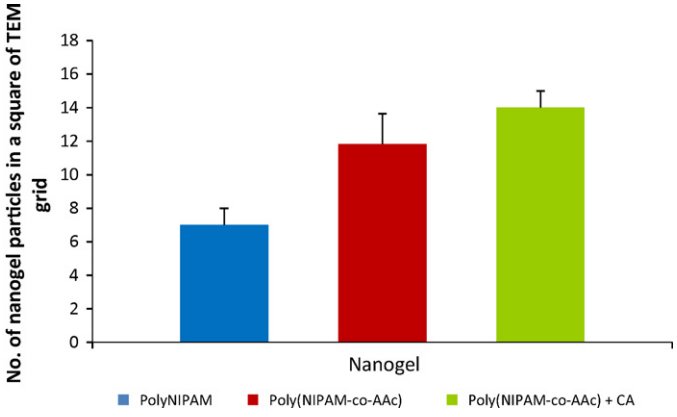

Fig. 8. Nanogel particles observed in the receptor phases by TEM 24 h post *in vitro* permeation test.

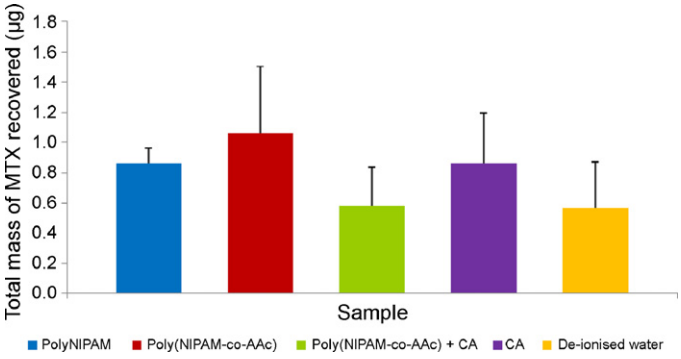

Fig. 9. Total mass of MTX recovered in the receptor phases after 24 h ($n = 3$, ±S.D.). Membranes were previously treated with polyNIPAM nanogel, poly(NIPAM-*co*-AAc) nanogel, poly(NIPAM-*co*-AAc) nanogels and CA (50 mg mL^{-1}), CA solution (50 mg mL^{-1}) and de-ionised water.

of the membranes by determining the permeation of the model drug, MTX, across the membranes used earlier. Although this is conventionally achieved by determining the flux of tritium (^{3}H), membrane integrity can also be indicated by demonstrating equal fluxes across a range of treatments. To this end, the *in vitro* skin permeation of MTX was probed to validate the integrity of the epidermal membranes post-application of nanogels and CA solution. Fig. 9 shows the total permeation of MTX after 24 h topical application of the saturated aqueous MTX solution onto the porcine epidermal membranes – any defects would be readily observed as significantly high amounts of MTX present. There was no significant difference ($p = 0.6478$) found in terms of MTX permeation between each group of epidermal membranes in comparison to the membranes dosed with de-ionised water (control). The solubility of MTX in PBS was 0.67 ± 0.007 mg mL^{-1} ($n = 3$, ±S.D.), approximately 1/700th of the levels found in the receptor phases, thus the data were not an artefact of solubility in the receptor phase.

4. Conclusion

To conclude, TEM images have revealed the first direct evidence that the polyNIPAM and poly(NIPAM-*co*-AAc) nanogels are able to penetrate the skin and migrate across the epidermis. The data go some way towards a mechanistic insight for the use of nanogels as drug carriers in topical drug delivery, although the events that

occur (i.e. the route) remain to be elucidated. Furthermore, the safety aspects of nanoparticulates potentially entering the systemic circulation via the topical route needs further study (Warheita et al., 2008), although there is some evidence that migration may be controllable to a certain extent.

References

Alvarez-Román, R., Naik, A., Kalia, Y.N., Fessi, H., Guy, R.H., 2004. Visualization of skin penetration using confocal laser scanning microscopy. Eur. J. Pharm. Biopharm. 58, 301–316.

Das, M., Zhang, H., Kumacheva, E., 2006. MICROGELS: old materials with new applications. Ann. Rev. Mater. Res. 36, 117–142.

de Jalón, E.G., Blanco-Príeto, M.J., Ygartua, P., Santoyo, S., 2001. Topical application of acyclovir-loaded microparticles: quantification of the drug in porcine skin layers. J. Control. Release 75, 191–197.

Don, T.-M., Huang, M.-L., Chiu, A.-C., Kuo, K.-H., Chiu, W.-Y., Chiu, L.-H., 2008. Preparation of thermo-responsive acrylic hydrogels useful for the application in transdermal drug delivery systems. Mater. Chem. Phys. 107, 266–273.

Dowding, P.J., Vincent, B., Williams, E., 2000. Preparation and swelling properties of poly(NIPAM) “minigel” particles prepared by inverse suspension polymerization. J. Colloid Interface Sci. 221, 268–272.

Galaev, I.Y., Mattiasson, B., 2007. Smart Polymers – Applications in Biotechnology and Biomedicine, 2nd revised ed. Taylor & Francis Ltd., Boca Raton, Fla, 496.

Hoare, T., Pelton, R., 2004. Functional group distributions in carboxylic acid containing poly(N-isopropylacrylamide) microgels. Langmuir 20, 2123–2133.

Lademann, J., Knorr, F., Richter, H., Blume-Peytavi, U., Vogt, A., Antoniou, C., Sterry, W., Patzelt, A., 2008. Hair follicles – an efficient storage and penetration pathway for topically applied substances. Skin Pharmacol. Physiol. 21, 150–155.

Lambers, H., Piessens, S., Bloem, A., Pronk, H., Finkel, P., 2006. Natural skin surface pH is on average below 5, which is beneficial for its resident flora. Int. J. Cosmetic Sci. 28, 359–370.

Lin, C.-L., Chiu, W.-Y., Lee, C.-F., 2006. Preparation, morphology, and thermoresponsive properties of poly(N-isopropylacrylamide)-based copolymer microgels. J. Polym. Sci. A: Polym. Chem. 44, 356–370.

Lee, C.-F, Lin, C. -C., Chiu, W. -Y., 2008. Thermosensitive and control release behavior of poly (N-isopropylacrylamide-co-acrylic acid) latex particles. J. Polym. Sci. A: Polym. Chem. 46, 5734–5741.

Leslie Singka et al., Leslie Singka, G.S., Samah, N.A., Zulfakar, M.H., Yurdasiper, A., Heard, C.M. in press. Enhanced topical delivery and anti-inflammatory activity of methotrexate from an activated nanogel. Eur. J. Pharm. Biopharm. In Press.

Oh, J.K., Drumright, R., Siegwart, D.J., Matyjaszewski, K., 2008. The development of microgels/nanogels for drug delivery applications. Prog. Polym. Sci. 33, 448–477.

Pelton, R.H., Chibante, P., 1986. Preparation of aqueous lattices with N-isopropylacrylamide. Colloids Surf. 20, 247–256.

Saunders, B.R., 2004. On the structure of poly(N-isopropylacrylamide) microgel particles. Langmuir 20, 3925–3932.

Schmidt, T., Janik, I., Kadlubowski, S., Ulanski, P., Rosiak, J.M., Reichelt, R., Arndt, K.-F., 2005. Pulsed electron beam irradiation of dilute aqueous poly(vinyl methyl ether) solutions. Polymer 46, 9908–9918.

Toll, R., Jacobi, U., Richter, H., Lademann, J., Schaefer, H., Blume-Peytavi, U., 2003. Penetration profile of microspheres in follicular targeting of terminal hair follicles. J. Invest. Dermatol. 123, 168–176.

Warheita, D.B., Sayes, C.M., Reed, K.L., Swain, K.A., 2008. Health effects related to nanoparticle exposures: environmental, health and safety considerations for assessing hazards and risks. Pharmacol. Ther. 120, 35–42.

Wu, X., Biatry, B., Cazeneuve, C., Guy, R.H., 2009. Drug delivery to the skin from submicron polymeric particle formulations: influence of particle size and polymer hydrophobicity. Pharm. Res. 26, 1995–2001.